0012-9402/04/010033-14
DOI 10.1007/s00015-004-1114-9
Birkhäuser Verlag, Basel, 2004

Eclogae geol. Helv. 97 (2004) 33–46

Late Neogene extension in the vicinity of the Simplon fault zone (central Alps, Switzerland)

GRÉGORY GROSJEAN, CHRISTIAN SUE & MARTIN BURKHARD

Key words: Central Alps, Simplon fault, brittle deformation, extension, late alpine tectonics

ABSTRACT

Brittle faults and kinematic indicators have been measured systematically below and above the major late alpine extensional Simplon fault in the vicinity of Simplonpass. Paleo-stress inversion has been conducted for a total of over 1200 fault measurements, from 62 sites. Minor faults in both hanging- and footwall of the Simplon fault define a coherent paleo-stress field with SW-NE oriented maximum horizontal extension and near vertical compression. The kinematics of these latest brittle deformations are in very good agreement with the ductile, slightly older deformations recorded within the Simplon fault mylonites (Mancktelow 1990). Paleo-stress orientations obtained from sets of the latest brittle faults are clearly different from the present day stress field as derived from earthquake focal plane mechanisms. The latter define a nearly N-S oriented maximum horizontal extension direction (Kastrup 2002), at a high angle to the downdip direction of the Simplon fault lineation. The present day stress orientation is ill orientatated for a reactivation of the Simplon fault and its associated minor fractures.

ZUSAMMENFASSUNG

Eine systematische Analyse von Sprödbrüchen ober- und unterhalb der Simplonstörung wurde in der Gegend des Simplonpasses durchgeführt. Die Inversion von über 1200 Bruchmessungen an 62 Messstationen erlaubt die Interpolation eines regionalen Paläo-Stressfeldes. Die gemessenen Sekundärbrüche sind weitgehend mit einem regional kohärenten Stresstensor zu erklären der eine SW-NE orientierte Streckung und eine nahezu senkrechte Kompression aufweist. Kinematisch passen diese späten Brüche sehr gut mit der etwas älteren, sehr intensiven plastischen Deformation der Mylonite entlang der Simplon Scherzone zusammen (Mancktelow 1990). Die Orientierung der Paläo-Stressachsen ist deutlich verschieden von der heute beobachteten Stressorientierung. Erdbeben-Herdflächenlösungen ergeben eine N-S orientierte Streckungsrichtung (Kastrup 2002), in einem grossen Winkel zur Lineation der Simplonstörung. Die heutige Stressorientierung ist demenstsprechend ungeeignet, um die Simplonstörung und die sie begleitenden Sekundärbrüche zu reaktivieren.

1. Introduction and Geological setting

The Simplon fault zone (SFZ) is a major extensional structure within the Central Swiss Alps (Mancktelow 1990). It separates the lower penninic nappes of the Ticino or "Lepontine" area to the east from a pile of higher penninic nappes to the west (Steck 1987, Escher et al. 1997). This classic tectonic terminology is a confusing understatement, however, since "penninic" does not refer to a common paleogeography of the different nappes (Fig. 1), but rather to a caracteristic deformation style. This terminology goes back to the first mapping efforts in this area (Gerlach 1883, Schmidt 1907, Schmidt & Preiswerk 1908) which soon led to the recognition of the superposition of basement nappes, separated from each other by thin layers of mesozoic metasediments (Lugeon 1903, Argand 1911). The nappe theory was nicely confirmed by the construction of the Simplon railway tunnel (Schmidt 1908, Milnes 1973). The so-called lower penninic nappes of the Ticino area, east of the Simplon fault are now identified as strongly deformed and metamorphosed basement slices derived from the southermost edge of the european, passive continental margin. Upper penninic nappes found to west of the Simplon fault are derived from the Briançonnais domain, a microcontinental "exotic terrane" separated from the European plate by the Valaisan ocean in late Mesozoic times (Stampfli & Marchant 1997). Primary nappe contacts have been obscured by complex polyphase tectonics (Keller & Schmid 2001). A first phase of northwestward directed nappe stacking has long been known to be followed by at least two phases of "backfolding", still in a general NW-SE collisional compression regime. Backfolding to the south is localized in two distinct regions: an Insubric phase of backfolding, associated with the Insubric line (Argand 1911, Schmid et al. 1987) and a "northern steep zone" at the southern rim of the external crystalline massifs (Milnes 1974). The oblique Simplon fault as a marked "anomaly" within this pile of supposedly "cylindrical" penninic nappes between Domodossola and the Simplon pass area, was discov-

Institut de Géologie, Université de Neuchâtel, Rue Emile-Argand 11, Case postale, CH–2007 Neuchâtel

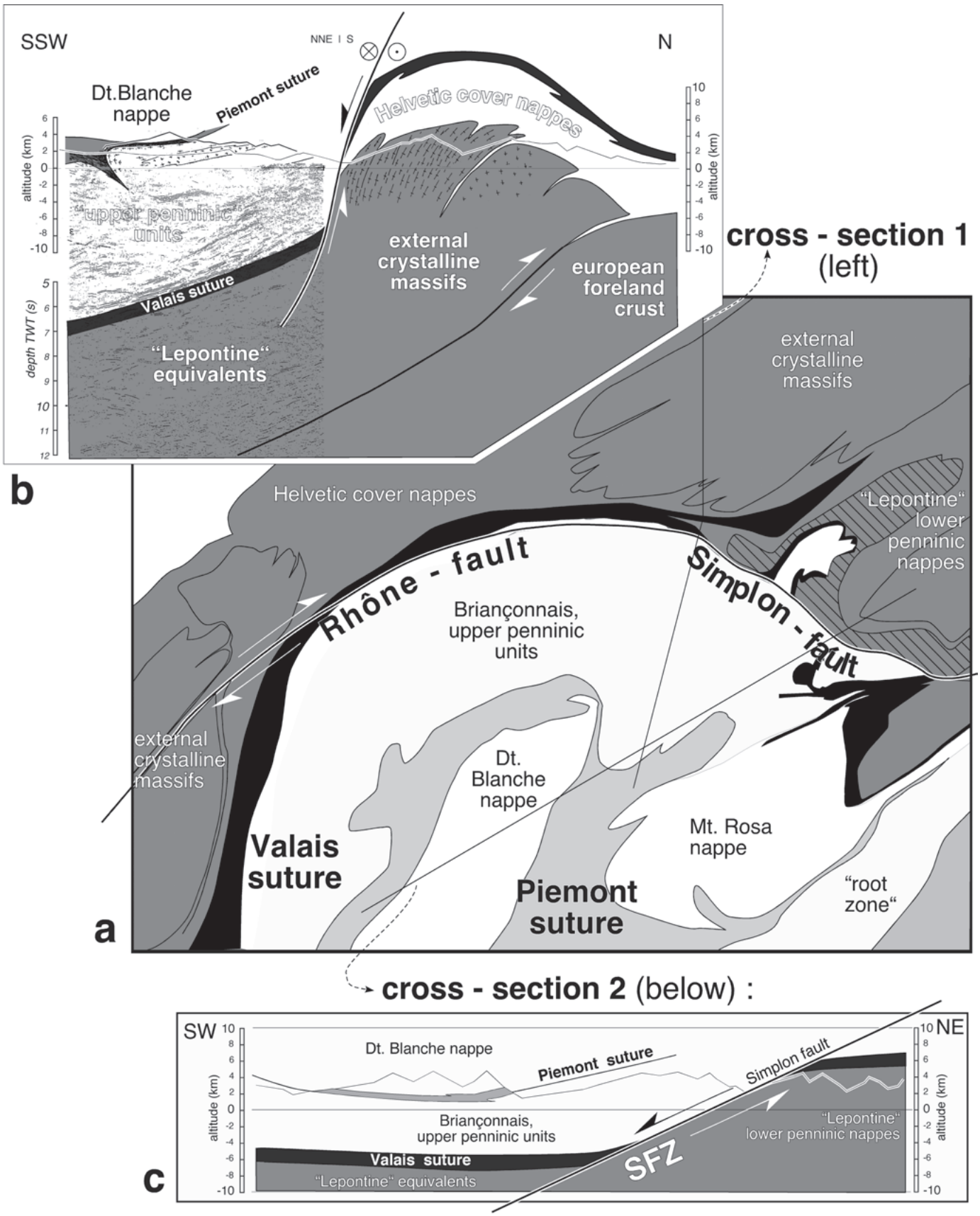
SSW
NNE I S
N
Dt.Blanche nappe
Piemont suture
Helvetic cover nappes
altitude (km)
depth TWT (s)
upper penninic units
external crystalline massifs
european foreland crust
Valais suture
"Lepontine" equivalents
b
cross - section 1 (left)
external crystalline massifs
Helvetic cover nappes
"Lepontine" lower penninic nappes
Rhône - fault
Simplon - fault
Briançonnais, upper penninic units
external crystalline massifs
Dt. Blanche nappe
Mt. Rosa nappe
Valais suture
Piemont suture
"root zone"
a
cross - section 2 (below) :
SW
NE
Dt. Blanche nappe
Piemont suture
Simplon fault
Briançonnais, upper penninic units
"Lepontine" lower penninic nappes
Valais suture
"Lepontine" equivalents
SFZ
c

ered relatively late (Amstutz 1954) and subsequently mapped in detail (Bearth 1956, 1972, 1973). The "Simplon fault" has since been identified as being just the brittle expression of a major ductile extensional shear zone. The cumulated horizonatal offset of the SFZ is on the order of 16 km in a transverse, SW-NE direction (Steck 1984, Mancktelow 1985, 1990). A large portion of this extension is accommodated within a one kilometer thick mylonitic horizon in the immediate footwall of the "Simplon fault". The kinematics of this mylonite zone have been worked out by detailed mapping and analysis of superimposed lineations and kinematic indicators (Mancktelow 1987, Mancktelow & Pavlis 1994). The SFZ appears as a late feature, which clearly post-dates nappe stacking by thrusting in a NW direction (Steck et al. 1989). The enormous thickness and the ductile nature of the Simplon mylonites are responsible for the apparent parallelism of nappe contacts with the brittle Simplon fault. This also explains the rather late discovery of this major transverse zone.

The SFZ seems to connect the southern and northern steep belts in an asymmetic sigmoidal open Z-shape in map view. It acts as a gently SW- dipping detachment fault, which cuts tectonic units out of section (Fig. 1b and c). In particular, the "suture" of the Valaisan ocean is virtually absent on the tectonic map of the Western Central Alps because it has been "removed" by the Simplon fault (Steck et al. 1999, Steck et al. 2001). In other words, the supposedly simple stack of superimposed nappes is not only modified by more or less co-axial backfolds but also, and more severely perturbed by the oblique SFZ. The classical method of cylindrical projection, introduced by Argand (1911) and widely applied ever since in order to construct "composite" cross sections through the Alps (Pfiffner et al. 1997), is invalid across such an oblique normal fault. This is one of the main reasons for the discrepancies prevailing among modern interpreted cross sections proposed across the Western Central Alps by various authors (Escher et al. 1987, Escher 1988, Jeanbourquin & Burri 1989, Mancktelow 1990, Steck et al. 1999, Steck et al. 2001). A better understanding of the SFZ and its role in the formation of the Central Alps might help to reduce such discrepancies.

At the scale of the Alpine orogen, the SFZ belongs to a family of late extensional features. This extension is clearly synchronous with ongoing Adria – Apulia convergence and thrusting in external alpine domains, however. "Orogenic collapse" in the course of, or slightly after collision tectonics has been predicted from theory and extensional structures have promptly been identified in many orogens worldwide (Dewey 1988, Platt et al. 1989). One of the most famous "type areas" for syn- to post-collisional extension is the Basin and Range province of the SW United States (Wernicke & Burchfiel 1982). The general concept of "metamorphic core complexes" has been applied to many other mountain chains, including the Alps. The Ticino "Lepontine dome" and the Austrian "Tauern window" bear similarities with the classic metamorphic core complexes of the Basin & Range (Selverstone 1988, Wawrzyniec & Selverstone 2001). In the case of the Lepontine "Ticino" dome, metamorphism was classically regarded as post-tectonic, since metamorphic isograds seem to crosscut nappe-internal structures (Niggli 1975, Trümpy 1980, Todd & Engi 1997). On the regional scale, however, the "Lepontine dome" of high grade metamorphism is surrounded by mylonite zones which affect both isograds and nappe-internal structures: to the south, high grade rocks of amphibolite zone are juxtaposed to lower greenschist facies rocks along the Insubric line, i.e. the footwall of this major backthrust. The northern limit of the amphibolite grade rocks coincides with the northern steep zone / backfold at the internal rim of the Gotthard massif. To the west, the domain of amphibolite facies abuts the SFZ. Last but not least, the eastern boundary of the high grade "Lepontine Ticino dome" has lately been shown to be cut by extensional faults quite "symmetrical" to the SFZ (Nievergelt et al. 1996). The simple picture of a post-tectonic "lepontine" metamorphic dome has thus disappeared in favour of a more complex history of pre- to syn-metamorphic nappe stacking and intense, partly superimposed folding, followed by syn- to post- post-peak metamorphic backfolding and simultaneous strike parallel extension / lateral extrusion (Steck & Hunziker 1994, Wawrzyniec & Selverstone 2001).

The details and origin of extensional structures in the Central Alps are still a matter of debate. Instead of advocating a post-orogenic collapse (e.g. Molnar & Lyon-Caen 1988), most alpine authors prefer lateral escape models in which sideways extrusion of crustal blocks is seen as a consequence of the shape and direction of an Adriatic indentor, pushing further into the already existing stack of alpine nappes during ongoing collision in Miocene times (Ratschbacher et al. 1989, Ratschbacher et al. 1991, Hubbard & Mancktelow 1992, Mancktelow 1992). Increasingly oblique compression with the development

Fig. 1a. Strongly simplified tectonic map of the Valais area (Steck et al. 1999). Lower plate units of european affinity are shown in gray, they include foreland crust, external crystalline massifs (Aar- and Gastern), lower penninic nappes of the "Lepontine" Ticino area and Helvetic cover nappes. Units of the northern, Valais "suture zone" are shown in black. Higher penninic units of the Briançon domain are left white. The main Piemontais suture zone (in gray) marks the separation between upper and lower plate of the Alpine collision. The Simplon Rhone fault system cuts across the alpine nappe stack in an oblique fashion, cutting out much of the Valais suture zone in the Simplon pass area.

b) Schematic N-S (NNE-SSW) cross section through the alpine nappe stack west of Simplon pass. This section follows the deep seismic reflexion profile W5 of NFP20 (Steck et al. 1997); this seismic lines does not extend to the north of the Rhone valley, but well marked reflectors "of upper penninic units" with a shallow southward dip abut against the steeply inclined foliation of the internal Aarmassif. We interpret this relationship with a major normal offset along the Rhone fault, the western continuation of the Simplon fault zone.

c) Schematic longitudial section across the Simplon fault in an ENE-WSW direction.

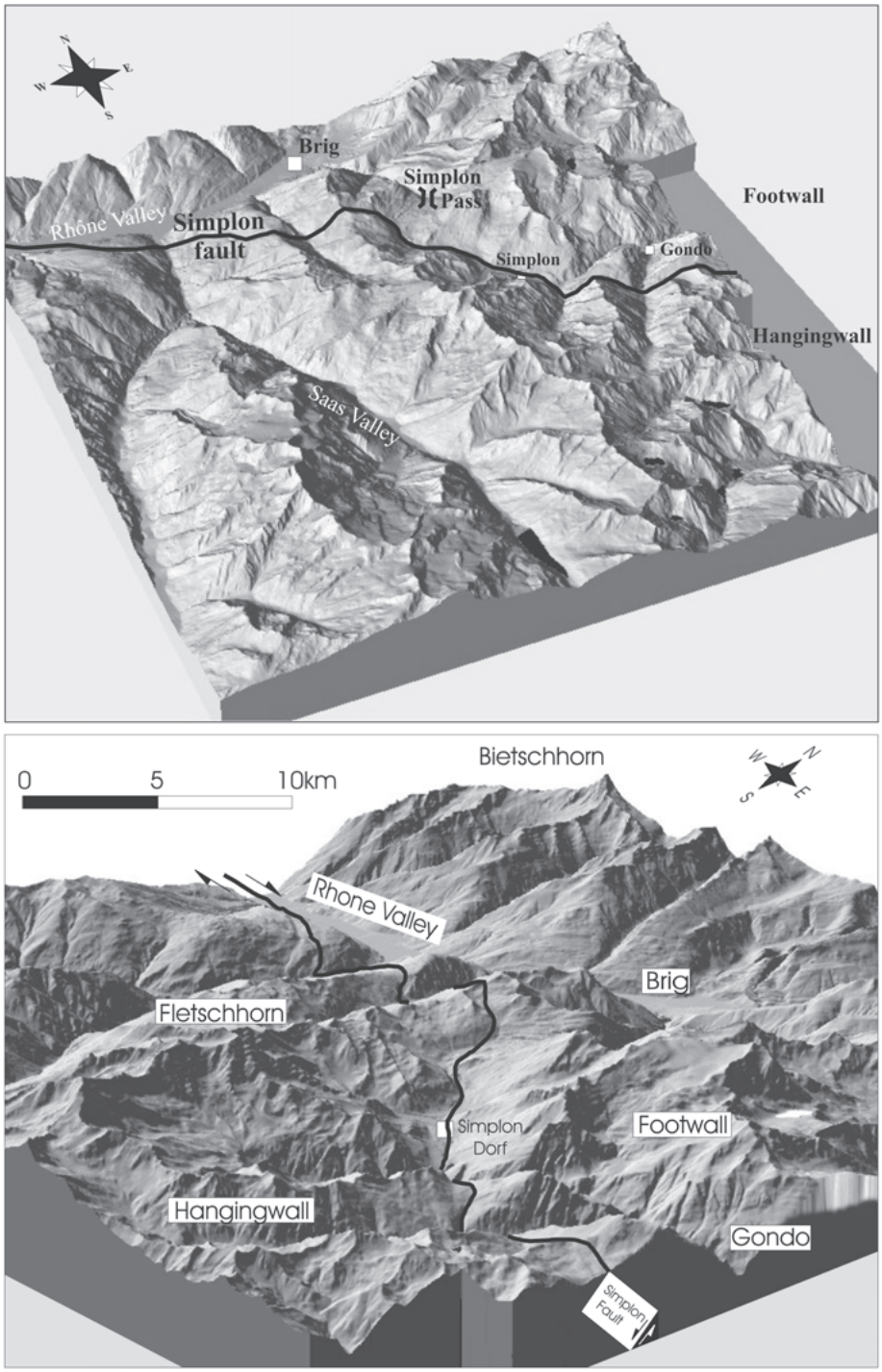

Fig. 2. Digital height model (DHM) of the studied area with location of the main branch of the Simplon fault. The fault presents a downthrow of the hangingwall to the SW, the footwall is exposed to the east of Simplon pass. The block diagrams are based on the MNT25 of swisstopo; permission BA046170.

of strike-slip faults and associated extension in "releasing bends" has long been advocated by Laubscher (1972, 1982, 1988, 1992).

Timing of the extensional activity along the SFZ is constrained by a large series of radiometric ages (Hunziker et al. 1997). The Simplon fault appears as a marked discontinuity in ages, determined by many methods applied to different minerals (K/Ar, Rb/Sr, Ar/Ar, zircon and apatite fission track). Ages determined in samples east of the SFZ are systematically younger than those from rocks of the higher penninic nappes sampled to the west. Such age differences have been used to model the timing of vertical displacements and associated cooling of the hanging- and foot-wall blocks on either side of the SFZ. It appears that a total vertical displacement on the order

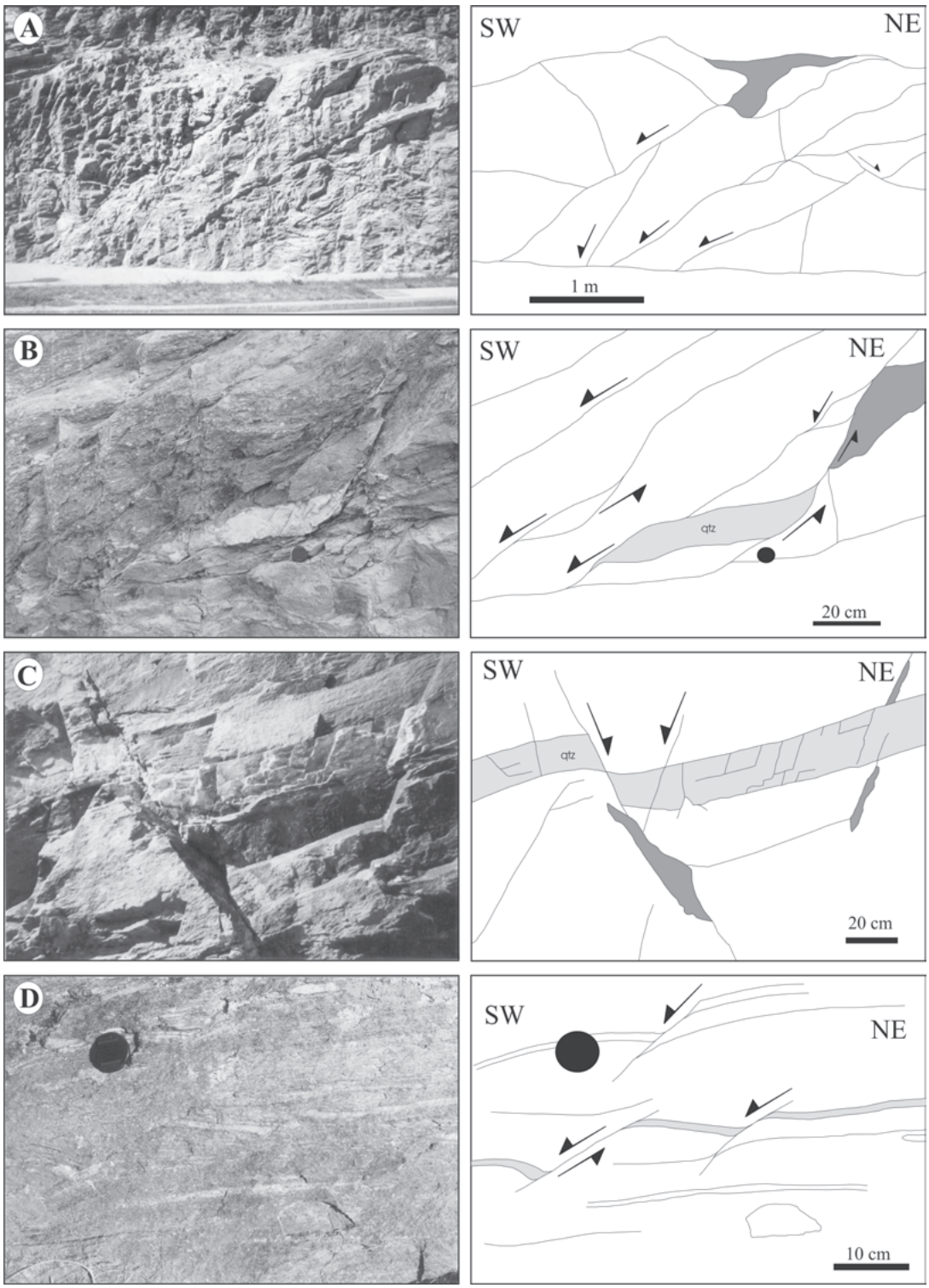

Fig. 3. Examples of late brittle extensional structures.
A) Post-mylonitic fault near Engiloch, Simplon road-cut, Monte Leone nappe. Mylonitic foliation, dipping at ca. 30° to the SW is cut by a later set of conjugate brittle normal faults.
B) Close up of outcrop shown in A. Feldspar clasts as well as asymmetrically sheared quartz veins indicate a normal "top to the SW" shear sense. At the right hand side (in dark grey on the sketch), a steep normal fault plane is mineralized with chlorite. Striations indicate a normal sense of shear.
C) Conjugate set of brittle normal faults. Engiloch, Simplon road-cut.
D) Normal faults in muscovite/biotite gneiss of the Lebendun nappe at Innri Alpa (north of the Gondo canyon) in the footwall of the SFZ.

of 7 km, associated with a horizontal displacement of at least 16 km took place between about 18 and 12 Ma (Mancktelow 1990). Such estimates stand and fall with the concept of "cooling ages", which has recently received some substantial criticism (Villa 1998). Apatite fission track (FT) ages are beyond such doubts, at least when applied to rapid cooling of high grade rocks from temperatures well above the partial annealing zone, i.e. 60 to 120°C in the case of apatite (Hurfond 1991). Apatite FT ages from the larger Simplon and Rhone valley area show systematically younger ages in the footwall of the Simplon-Rhone fault system (Soom 1990, Seward & Mancktelow 1994) than in the hangingwall of the upper Penninic nappes. These data provide strong evidence for continued faulting activity as young as 5 to 3 Ma, considerably younger than previous estimates (Mancktelow 1990). Thermal modelling has been used to further constrain possible P-T-t curves for rocks on either side of the SFZ (Grasemann & Mancktelow 1993).

In maps of the present day seismic activity, the Simplon area appears as a region of quiescence. In contrast, the central Valais area, some 10 to 50 km further to the west, is one of the most seismically active zones of Switzerland in particular and the Western Alps in general (Deichmann et al. 1998). Two distinct present-day stress regimes have been identified on either side of the Rhone valley from the inversion of fault plane solutions (Maurer 1993, Maurer et al. 1997). A dextral strike-slip regime with a slight component of extension prevails in the Rawil saddle, north of the Rhone valley, but mostly concentrated along a subvertical WSW-ENE lineament running below the Rawil saddle. The higher penninic nappes south of the Rhone valley display an extensional regime with a slight component of strike-slip, with hypocenters widely distributed throughout the entire volume of upper penninic crust. In contrast to kinematic data from the SFZ mylonites with a SW-NE extension, the present day stress regime in the hangingwall of the Rhone – Simplon fault zone indicates a N-S oriented extension.

In this paper we examine late brittle deformation features on either side of the Simplon fault. Using well established techniques of fault/striae measurements and their inversion (Angelier 1994), we mapped paleo-stress directions and regimes in the larger Simplon area. Given the late, clearly post-mylonitic age of these brittle faults, their analysis allows to bridge the gap between the well studied kinematics of the SFZ mylonites (Mancktelow 1990) and the present day stress regime as known from the inversion of earthquake data (Maurer et al. 1997, Kastrup 2002). Faults and systematic joint sets are ubiquitous and well exposed in rocky outcrops of the high alpine area around the Simplonpass and the Gondo gorge. Larger faults as well as systematic joint sets generally appear as geomorphic features such as gullies and cliffs. We conducted an intense search for very young, post-glacial activity of such faults in an area SW of the Simplon pass, i.e. in the SW prolongation of the Simplon fault, in the field as well as using aerial photography and digital elevation models (Fig. 2).

2. Faults, joints and associated brittle microstructures

Minor faults are ubiquitous in the gneisses adjacent to the SFZ, their length ranges from some dm to several hundreds of meters, exceptionally kilometers. Absolute offsets are on the scale of cm to dm in the case of smaller faults seen in road-cuts and other fresh outcrops; absolute offsets are very difficult or impossible to determine on the larger, map scale faults. A series of nice examples of out-crop scale, post-mylonitic brittle fault structures are shown in Fig. 3.

In order to be useful for structural studies and paleo-stress determinations, the following measurements have to be made on individual minor faults: 1) orientation of fault plane, 2) orientation of fault movement (slickenside), 3) sense of shear. Sense of shear determination on brittle faults is facilitated by the presence of syn-tectonic fiber growth, often in a characteristic asymmetric stepping pattern (Petit 1987, Ramsay & Huber 1987). The most common minerals found on fault planes in the Simplon area are quartz, chlorite, epidote, (Fe-) calcite, dolomite and occasionally hematite. In most cases, only two, exceptionally three minerals out of this set are present on any individual fault plane. In some rare cases, deep within the footwall, faults and associated veins contain also white mica. Additional brittle shear sense indicators include asymmetric grooves, wear marks, secondary Riedel shears, en échelon tension gashes and so forth (Petit 1987). Shear sense determination is the most difficult and often impossible in the case of very planar, nicely polished fault "mirror" surfaces. Polished fault mirrors are always associated with sub-millimetre to dm thick seams of cataclasites and/or ultracataclasites. In contrast to fault planes decorated by mineral fibers, cataclastic faults in general and fault mirrors in particular are thought to be the latest expression of extensional tectonics that took place at low to very low temperatures. We have not been able to identify any true pseudotachilites in the Simplon area, nor have such structures been reported in the literature (Mancktelow 1990, Wawrzyniec & Selverstone 2001).

The Simplon fault itself is nicely expressed as a geomorphic feature in the field (Fig. 4). The gently dipping brittle fault is clearly less resistant to erosion than the footwall mylonites. The fault plane itself can never be completely observed in outcrop; closest outcrops are at metric distance, however, and display very intense cataclastic to ultracataclastic deformation. In one sub-outcrop in Zwischbergtal, a white clay fault gouge is "seeping" out of the supposed master fault. This plastic gouge material is composed of >90% illite (XRD determination), with sub-micrometer grain size (from centrifuge settling experiments, Stoke's law) with sparse, highly angular quartz-grains and rock fragments of larger, up to cm size. Similar occurences of clay gouges are reported from the Simplon railway tunnel and road tunnels near Crevola Dossola (A. Parriaux, EPFL Lausanne, oral communication 1999).

A marked contrast in macroscopic rock fabric is observed between the foot- and hangingwall of the Simplon fault (Mancktelow 1990). The footwall is characterized by a very

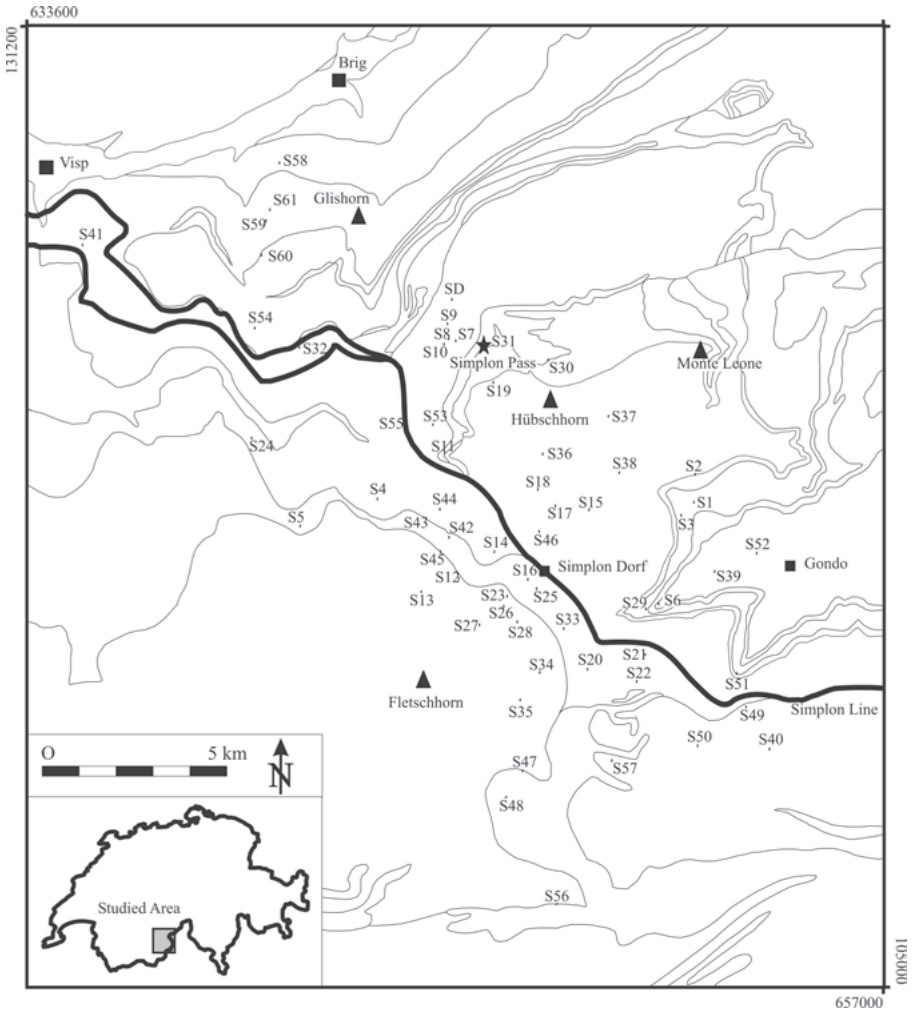

Fig. 4. Location of the 62 measurement sites.

regular planar mylonitic foliation, which runs subparallel to the Simplon fault. This foliation dominates the morphology of the region east of the Simplon fault, where summits have gentle dipslopes facing southwest and steep cliffs facing northeast. In contrast, the hangingwall, west of the Simplon fault is much less foliated and has a more blocky, irregular appearance. Summits west of the Simplon fault are symmetrical "horns" with no marked influence of foliation on their morphology. Both foot- and hangingwalls display a sufficient number of minor faults for the reconstruction of paleo-stress-tensors. No obvious difference in orientation, appearance or mineralogy of minor fault surfaces has been detected between hanging- and foot-wall of the SFZ.

Systematic joint sets are more prominent in the footwall than in the hangingwall. Macroscopically, joints are distinguished from faults by the absence of displacements other than normal to the fracture surface and by their occurence in sets of many individual, variably spaced fracture surfaces with identical orientation (Hancock 1985, Dunne & Hancock 1994). Close inspection of joint surfaces reveals many of them to be re-utilized in shear, however: they are striated and often mineralized with quartz, chlorite, epidote and hematite. Accordingly, the distinction between faults and joints is not always straightforward and nicely striated original joint surfaces have been included in our fault/striae measurements.

3. Data analysis

In order to determine local paleo-stress directions, we used classic methods of stress-inversion; for an indepth discussion see (Angelier & Mechler 1977, Angelier 1994). Numerical methods for paleostress tensor inversion are based on the assumption that measured striations and shear sense from many individual fault surfaces are a record of a single overall stress tensor responsible for slip on these surfaces. Resolved shear stress orientation on each fault surface is assumed to be parallel to the measured slip vector (Wallace 1951, Bott 1959). Given a large population of individual fault/striae measurements from any single outcrop, ideally with many conjugate sets of faults and some spread in fault orientations, inversion methods allow to search for the overall stress tensor which yields the best fit between theoretically predicted slip direc-

Tab. 1. Parameters for the paleostress presented on Fig. 6.
For a given site, **code** and **site** refer to the measurement site. **X**, **Y** are the Swiss coordinates, **Z** the altitude of the measurement site. The number of data inverted is **n**; **m** is the average angle between the measured and computed striae (calculated for each data); s is the standard deviation of the these angles; σ_1, σ_2, σ_3 give the orientation (azimut, plunge) of the main stress axes; RΦ is the shape ratio for the stress tensor ellipsoid [$R\Phi = (\sigma_2-\sigma_3)/(\sigma_1-\sigma_3)$].

Code	Site	X	Y	Z (m)	n	m	s	σ_1	σ_2	σ_3	Rϕ
S1	Innri Alpa	651500	118175	1660	13	5.8	4.3	312 / 69	125 / 21	216 / 02	0.3
S2	Schwarzi Balma	651525	118525	1980	13	10.3	8.1	124 / 72	351 / 12	258 / 13	0.3
S3	Innri Biela	651275	117750	1720	10	6.9	6.1	300 / 80	129 / 10	038 / 02	0.6
S4	Sirwoltensee	642950	118200	2400	9	5.8	4.5	348 / 74	222 / 10	129 / 13	0.2
S5	Obers Fulmoos	640850	117450	2460	10	7.9	7.6	357 / 63	159 / 26	253 / 07	0.6
S6	Alte Kaserne	650725	115400	1180	17	5.8	5.3	149 / 82	326 / 08	056 / 01	0.4
S7	Hopschusee	645075	122575	2020	10	6.4	3.8	110 / 81	322 / 07	232 / 05	0.6
S8	Hopschusee	644925	122600	2060	13	6.2	3.6	128 / 70	336 / 17	243 / 09	0.9
S9	Staldhorn	644850	123000	2200	11	12.0	8.3	135 / 63	334 / 26	240 / 08	0.5
S10	Hopsche	644800	122425	2060	15	7.2	7.1	039 / 87	138 / 01	228 / 03	0.8
S11	Engiloch	644800	119375	1800	46	11.5	7.6	090 / 80	329 / 05	238 / 09	0.5
S12	Rossbodestafel	645175	116050	1980	21	11.8	8.8	010 / 80	134 / 06	224 / 08	0.4
S13	Gali Egga	644125	115625	2360	18	18.2	10.1	240 / 85	133 / 01	043 / 04	0.3
S14	Egga	646075	116925	1720	29	9.7	9.2	303 / 73	050 / 05	141 / 17	0.4
S15	Glatthorn	648750	117900	2360	21	8.5	7.1	174 / 75	325 / 13	056 / 07	0.6
S16	Bodme	647275	115700	1750	16	6.0	6.8	219 / 83	309 / 00	039 / 07	0.3
S17	Walderuberg	647750	118000	2110	17	8.4	5.4	134 / 82	337 / 07	246 / 03	0.5
S18	Homatta	647300	118450	1940	13	5.7	4.9	128 / 67	352 / 17	257 / 15	0.2
S19	Hübschhorn W	646100	121400	2160	17	9.7	6.8	101 / 74	325 / 12	232 / 11	0.7
S20	Biel	648700	113500	1420	42	10.8	7.3	000 / 69	117 / 10	211 / 18	0.2
S21	Furggu	650250	113975	2000	9	13.6	12.2	161 / 75	324 / 15	056 / 04	0.7
S22	Guggilihorn	650000	113200	2120	14	8.8	10.0	356 / 56	222 / 18	126 / 17	0.0
S23	Bodmerhorn	646450	115525	2100	17	6.9	4.7	070 / 72	302 / 12	209 / 14	0.3
S24	Ochseläger	639550	119850	2340	31	10.0	7.2	066 / 77	285 / 10	194 / 08	0.2
S25	Lawigrabe	647000	116000	1800	43	10.3	7.8	054 / 73	186 / 12	279 / 12	0.1
S26	Bodmerhorn	646325	115225	2240	31	9.0	5.8	103 / 73	329 / 12	237 / 12	0.2
S27	Bodmergletscher	645675	114750	2520	27	9.4	7.4	085 / 75	320 / 09	228 / 12	0.3
S28	Blauseewji	646700	114850	2210	12	14.5	9.1	016 / 81	171 / 08	262 / 04	0.2
S29	Alte Kaserne	650225	115150	1200	26	9.8	6.8	151 / 83	315 / 07	045 / 02	0.5
S30	Chaltwasser	647525	122000	2280	47	9.4	6.8	081 / 76	333 / 05	242 / 14	0.3
S31	Simplon - Kulm	645875	122325	2000	12	6.2	4.5	106 / 77	325 / 10	234 / 08	0.5
S32	Stockji	640850	122375	2130	15	5.1	5.0	066 / 86	288 / 03	198 / 03	0.4
S33	Antonius	648050	114600	2060	30	14.0	7.7	093 / 77	348 / 04	257 / 12	0.3
S34	Färicha	647250	113450	2260	27	7.9	5.7	308 / 79	125 / 11	215 / 01	0.4
S35	Laggin Biwak	646775	112700	2430	21	9.9	7.2	072 / 74	200 / 10	292 / 12	0.1
S36	Hübschhorn S	647450	119400	2250	34	8.6	5.6	067 / 73	332 / 02	242 / 17	0.2
S37	Breithorn	649250	120400	2920	27	5.7	4.9	083 / 73	335 / 05	243 / 16	0.3
S38	Chesselhorn	649550	118900	2930	15	8.9	4.4	150 / 64	006 / 21	270 / 14	0.4
S39	Casermetta	652125	116175	1050	17	7.2	4.2	012 / 87	137 / 02	227 / 03	0.5
S40	Waira	653550	111375	2200	34	12.7	8.5	257 / 71	350 / 01	081 / 19	0.3
S41	Stalden	635000	125200	850	15	12.7	11.5	056 / 76	325 / 01	235 / 14	0.2
S42	Furgghalte	644900	117150	2260	24	9.9	6.5	166 / 76	316 / 12	047 / 07	0.5
S43	Schilthorn	644225	117700	2560	15	6.8	6.5	242 / 73	334 / 01	065 / 17	0.1
S44	Wyssbode	644625	117875	2400	12	9.5	7.0	284 / 70	024 / 04	116 / 20	0.4
S45	Obre Stossbode	644650	116775	2320	9	9.6	7.4	238 / 85	341 / 01	071 / 05	0.3
S46	Holiecht	647375	117300	1750	26	8.3	7.5	174 / 85	322 / 05	052 / 03	0.4
S47	Gärtjini	646850	110850	2260	27	11.2	6.9	148 / 76	332 / 14	242 / 01	0.3
S48	Weissmiesgletscher	646450	110050	2620	19	7.6	3.9	180 / 80	344 / 09	074 / 02	0.3
S49	Schafnuwald	652900	112475	1630	21	9.1	5.6	337 / 74	147 / 15	237 / 03	0.2
S50	Tannuwald	651650	111475	1520	10	7.2	2.3	190 / 77	026 / 12	295 / 03	0.6
S51	Sera	652688	113375	1300	9	8.0	6.7	005 / 80	160 / 10	250 / 04	0.5
S52	Ramserna	653225	116675	1000	19	7.5	5.6	030 / 76	134 / 04	224 / 14	0.4
S53	Altes Hospiz	644475	120275	1900	27	10.0	6.8	121 / 73	322 / 16	230 / 06	0.2
S54	Nidristi Alp	639725	122925	1720	21	7.9	6.6	130 / 75	325 / 15	235 / 04	0.8
S55	Gampisch	643650	120225	1930	11	6.6	2.9	009 / 75	140 / 10	232 / 11	0.2
S56	Zwischbergen Gletscher	647525	107375	2520	10	12.2	9.3	165 / 56	340 / 34	071 / 03	0.2
S57	Galaberr	649300	111125	2100	19	7.9	4.7	024 / 72	203 / 18	293 / 01	0.3
S58	Glis	640325	127425	1190	11	8.9	4.0	356 / 69	091 / 02	181 / 21	0.3
S59	Mäderhitta	639975	125813	1340	18	11.3	8.1	012 / 75	281 / 01	191 / 15	0.1
S60	Mäderhitta	639863	124975	1440	26	13.0	8.4	114 / 86	248 / 03	338 / 03	0.3
S61	Griewald	640025	126150	1330	13	15.8	7.4	001 / 87	227 / 02	137 / 02	0.2
SD	Staldhorn	644950	123700	2390	11	9.7	8.2	145 / 04	357 / 85	235 / 02	0.7

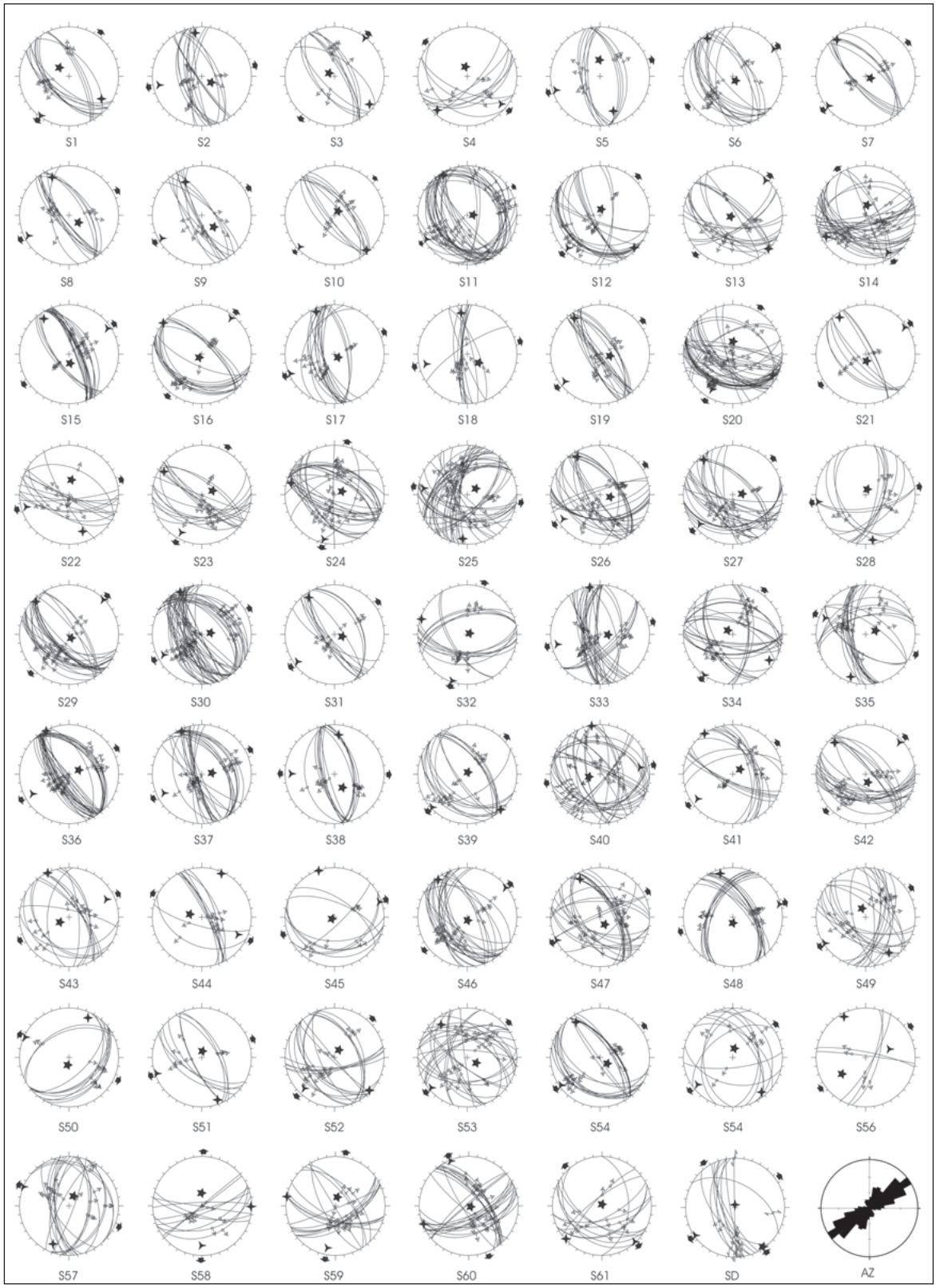

Fig. 5. Stereonets (equal area projection, lower hemisphere) of the 62 paleostress tensors computed in this paper. Each stereonet provides the fault orientation (great circles), the striae (marked on the great circle) as well as the best fit paleostress tensor obtained by inversion. Stars with 5, 4, and 3 branches stand for σ_1, σ_2, and σ_3 axis respectively. The code below each stereonet refers to the site listed in table 1.

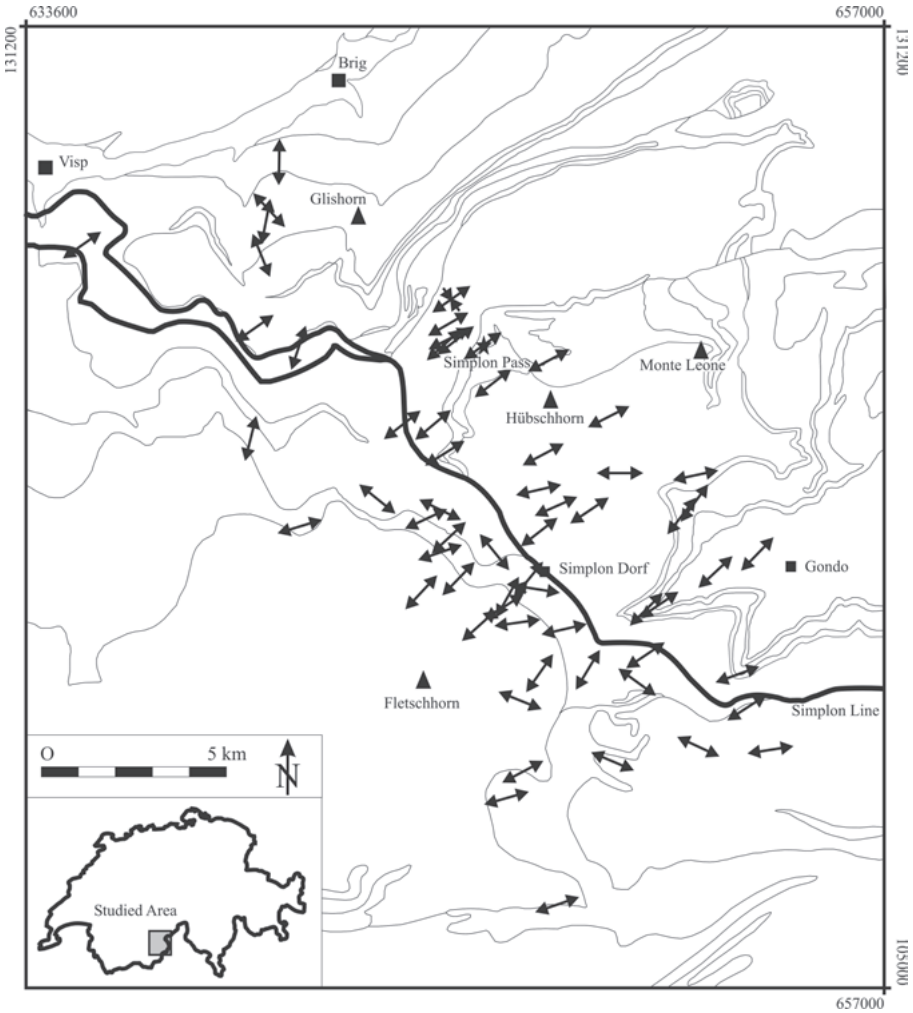

Fig. 6. Kinematics of the brittle extension in the studied area. Arrows show the projection on the map of the computed σ_3 axis for the extensional paleostress tensors. We computed one strike-slip paleostress tensor at the site sd for which both σ_1 and σ_3 axis projections are plotted.

tions on the measured striations on fault planes. Angular misfits are minimized by varying simultaneously both the orientation of the stress tensor (i.e. the directions of principal axes σ_1, σ_2 and σ_3) and the shape ratio of the stress ellipsoid $\Phi=(\sigma_2-\sigma_3)/(\sigma_1-\sigma_3)$.

A series of stress inversion methods have been proposed, mostly by the french school lead by Angelier (Angelier & Mechler 1977, Angelier 1994). Here we used the Direct Inversion method *INVD* (Angelier 1990)), which solves analytically the inverse problem of the paleostress tensor, using the *STRESS* software (Villemin & Charlesworth 1992). All stress inversion methods make a series of assumptions which are difficult to verify: homogeneity and isotropy of the rock volume, uniformity of the stress field, free slip along fault planes, small total finite strain, negligible passive rotation of fault planes (and adjacent wall rocks) with progressive deformation etc. Nevertheless, the quality of the resultant mean stress is justified *a posteriori* by the coherency of the obtained results. This coherency is obvious in graphical representations of fault dihedra superposition plots (Angelier & Mechler 1977); more sophisticated inversion programs calculate a series of parameters such as the total of angular misfits and standard deviations on orientation data which provide good estimates for the quality of the results. In cases where many ill-oriented fault/striae pairs are present in a fault population, the separation of faults into two or more subsets is to be considered. The observation and/or verification of polyphased paleostress results relies on structural criteria, however, such as cross-cutting relationships between generations of faults and/or striations on a fault.

We present a novel set of paleo-stress determinations conducted in 62 sites (Fig. 4) based on a total of over 1200 individual fault-striae measurements from the larger Simplon pass area. Key data for each measurement site are listed in Table 1. Raw data, *i.e.* fault orientations are visualized in the form of stereographic projections in Fig. 5 together with the best fit paleo-stress tensor obtained for each site. These data reveal the predominance of an extensional paleo-stresse regime, with subvertical σ_1 and subhorizontal σ_2 and σ_3 axes. There is only one exception to this rule, site SD, which displays a strike-slip regime (σ_2 vertical). For most of the tensors, the number of faults used for paleo-stress inversion as well as the average misfit angle between measured and computed striation, indi-

cate a good quality of inversion. Note that only few data have been rejected during the inversion process (typically less than 10%), and that no automatic sorting has been used. Some important variations exist in the Φ ratio, *i.e.* in the shape of the stress ellipsoid, with no obious regionalization. This ratio ranges from 0,1 to 0,9, with a mean value of 0,37, and a distribution rather close to a classical gaussian. Regional variations in the orientation of the subhorizontal extension axis (σ_3) are shown in Fig. 6. This map shows a highly consistent SW-NE trend for the major extension direction, *i.e.* the σ_3 axes. A slight deviation from this trend to a more N-S orientation is observed to the north, near Brig. Some apparent outliers, with a NW-SE direction (e.g. sites S4, S22, S35, S44, S50, S57) have low Φ ratios. This could be an indication for a weak difference between σ_2 and σ_3; i.e. a stress ellipsoid with a circular symmetry around the well defined subvertical σ_1 axis. In this case, permutation between σ_2 and σ_3 is commonly observed, and extension directions are ill defined. They could also correspond to a second order NW-SE stress field, weaker than the first order NE-SW one in terms of imprint in the field. Some tensors may also correspond to the mixing of two tensors corresponding to NE-SW and NW-SE extensional directions in the same site (e.g. S14, S23, S25, S27, S59, S60). We did not separate such datasets, as we tried to keep our analysis as simple as possible. Our global paleostress field is consistently NE-SW, but a weaker NW-SE extensional field could also been inferred from our data, which is illustrated by the σ_3 stereonet of the Fig. 7. Note that the computed or potential NW-SE extensional direction concerns less than 15% of the tensors of our database. In summary, near the Simplon fault zone, we obtained a very consistent set of paleostress tensors showing a regionally coherent NE-SW extension.

The high regional consistency of the data-set is further confirmed by some statistical representations of selected aspects of the orientation data (Fig. 7). The average extension direction (σ_3) of all measured sites taken together is 241°/04°; this orientation is very close to the average azimuth (line of maximum dip) 232° of all measured fault planes (Fig. 8). This close correspondence indicates the predominance of dip-slip normal faults. The stereogram of the σ_3-axes shown in Fig. 7 shows a slight preference for SW dipping σ_3 axis over those dipping gently to the NE. The distributions of the σ_1 (vertical) and σ_2 (perpendicular to σ_3) axes corroborate the very consistent extensional paleo-stress field in the NE-SW direction. Note that the concentration of stress axes around the mean values underlines the regional stability of the paleo-stress field.

All these data indicate a SW-NE oriented subhorizontal extension. This orientation is very close to the average SW plunging lineation measured in SFZ mylonites: 243°/25° (Mancktelow 1990, Fig. 24).

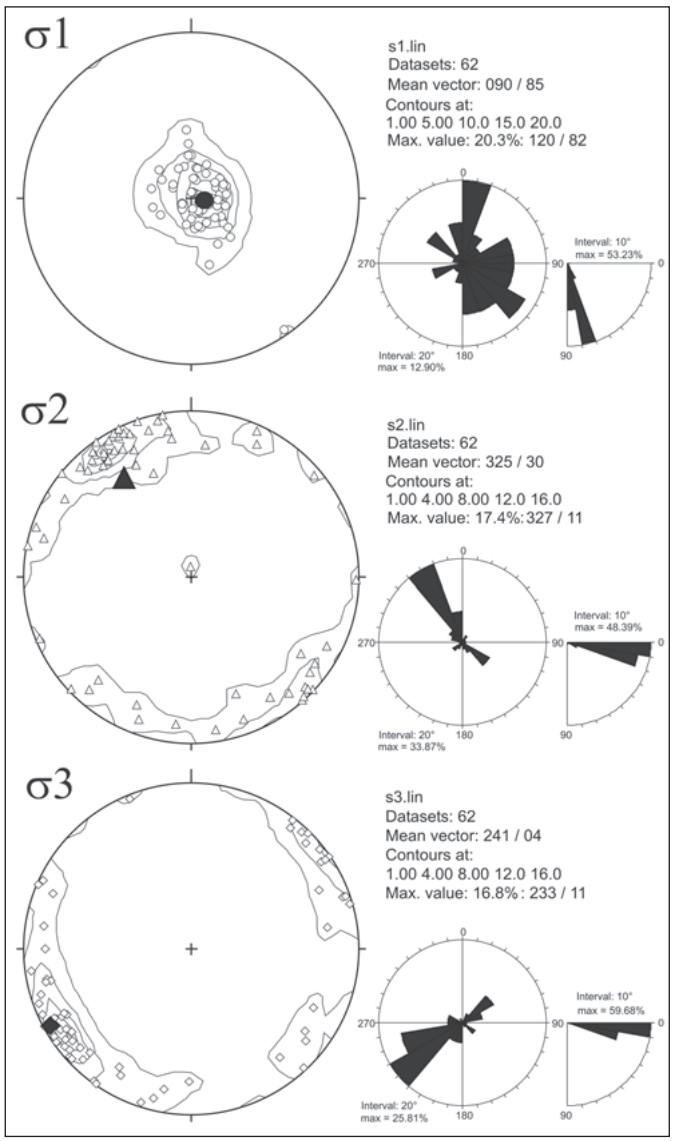

Fig. 7. Statistical distribution of the stress axes computed for 62 measurement sites (equal area projection, lower hemisphere), with the corresponding density contour diagrams. Note the coherent sub-vertical orientation of σ_1 with both σ_2 and σ_3 sub-horizontal.

4. Discussion and conclusion

The main result of our study is the characterization of the late-alpine brittle deformation in the vicinity of the Simplon fault, in the Central Swiss Alps. We obtained a very coherent paleostress field with a subhorizontal NE-SW oriented extension direction. Brittle deformations and kinematics are in very good agreement with the ductile, slightly older extension described in this area (Mancktelow 1990). We propose a tectonic continuum between the ductile extension responsible for the Simplon mylonite zone and the brittle deformation described in this paper. This relationship also leads to propose a continuity in terms of dynamic processes, which seem to rule the extensional tectonics in the central Alps (Sue & Tricart 2002).

A NE-SW direction of extension, under brittle conditions, has also been found in the Aosta and Ossola Valleys, to the

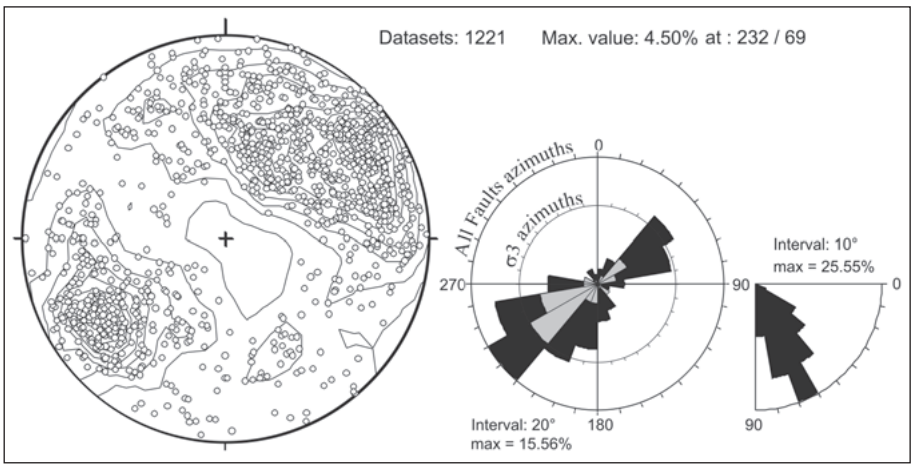

Fig. 8. Stereographic representation of all the fault measurements used in this study, with the corresponding density diagrams (equal area of the poles of the plane projections, lower hemisphere). The maximum density value is obtained at (az=232; pl=69).

SW of the Simplon fault zone (Bistacchi et al. 2000, Bistacchi & Massironi 2000). The same kind of brittle extension is also described by Champagnac et al. (2003) in the Valais area, immediately to the West of the Simplon fault Zone. Simplon fault kinematics and their associated NE-SW direction of extension thus appears as a major, widespread feature of late-alpine tectonics of the northwestern inner Alps. Simplon-like kinematics controlled the regional tectonics of a large area in the northwestern Alps in at least Late Neogene times, far westerward and southwestward of the Simplon fault proper.

In comparison with the present day stress field as determined from earthquake analyses in general and focal mechanisms in particular, the NE-SW direction of extension described in the whole Simplon-Valais-Aosta area is no longer active today. The Simplon area itself is seismically quiet today. Nevertheless, the larger Valais area is one of the most seismically active zones of the Alps. The strain/stress analyses performed in this area (Maurer 1993) and at ther larger scale (Sue et al. 1999, Kastrup 2002) clearly indicate a present day extension in a N-S direction, at a high angle to the strike of the chain. Such a radial extension seems to be active all along the internal parts of the northwestern Alps today. There seems to be an evolution in terms of stress field orientation with time. Qualitatively, extension remains the main feature of the paleo- and ongoing stress field in this part of the alpine belt. Quantitatively, however, the stress field in the Valais area evolved from NE-SW direction of extension during the Neogene to a N-S direction of extension in more recent times. The question remains open if this evolution represents a continuum in terms of geodynamic processes, or if the change in extensional direction represents a more dramatic rupture in the dynamics within the Alpine thrust belt.

In conclusion, our study allowed to precisely map the paleo-stress field associated with the latest stages of brittle deformation associated with the Simplon fault zone. The NE-SW extension described here is in continuity with the ductile extension along this major alpine normal fault. Moreover, it seems that Simplon-like kinematics ruled the tectonics of a very large Simplon-Valais-Aosta area during Neogene times. Considering the ongoing activity of the belt, there is a discrepancy between the Neogene extensional paleo-stress field and the present day still active N-S extension in the northwestern Alps.

Acknowledgements

We wish to thank Neil Mancktelow, Jane Selverstone, Jean-Daniel Champagnac, and Bastien Delacou for many fruitlul discussions. We are grateful to A. Bistacchi and O. Lacombe for constructive reviews. This work is part of the ongoing Swiss National Found project n° 21-61684.00.

REFERENCES

Amstutz, A. 1954: Pennides dans l'Ossola et problème des racines. Arch. Sci. Genève 7, 411 p.

Angelier, J. 1990: Inversion of field data in fault tectonics to obtain the regional stress; Part 3, A new rapid direct inversion method by analytical means. Geophys. J. Int. 103/2, 363–376.

– 1994: Fault slip analysis and paleostress reconstruction. In: Hancock, P. L. (Eds) Continental Deformation. Pergamon Press, Oxford, 53–100.

Angelier, J. & Mechler, P. 1977: Sur une méthode graphique de recherche des contraintes principales également utilisable en tectonique et en séismologie: la méthode des dièdres droits. Bull. Soc. Géol. France 19/6, 1309–1318.

Argand, E. 1911: Les nappes de recouvrement des Alpes Pennines et leur prolongements structuraux. Matér. Carte Géol. Suisse [n.s.] 31, 26p.

Bearth, P. 1956: Geologische Beobachtungen im Grenzgebiet der lepontinischen und penninischen Alpen. Eclogae geol. Helv. 49, 279–290.

– 1972: Simplon, Schweiz. Geol. Komm., Geol. Atlas Schweiz, 1: 25'000, Blatt 61.

– 1973: Erläuterungen zu Blatt Simplon (Atlasblatt 61),

Bistacchi, A. & Massironi, M. 2000: Post-nappe brittle tectonics and kinematic evolution of the north-western Alps; an integrated approach. Tectonophysics 327/3–4, 267–292.

Bistacchi, A., Eva, E., Massironi, M. & Solarino, S. 2000: Miocene to present kinematics of the NW-Alps; evidences from remote sensing, structural analysis, seismotectonics and thermochronology. J. Geodyn. 30/1–2, 205–228.

Bott, M. H. P. 1959: The mechanics of oblique slip faulting. Geol. Mag. 96/2, 109–117.

CHAMPAGNAC, J. D., SUE, C., DELACOU, B. & BURKHARD, M. 2003: Brittle orogen-parallel extension in the S. Valais. Eclogae geol. Helv. 96/3, 325–338.

DEICHMANN, N., BAER, M., DOLFIN, D. B., FAEH, D., FLUECK, P., KASTRUP, U., KRADOLFER, U., KUENZLE, W., MAYER-ROSA, D., ROETHLISBERGER, S., SCHLER, T., SELLAMI, S., SMIT, P. & GIARDINI, D. 1998: Earthquakes in Switzerland and surrounding regions during 1997. Eclogae Geol. Helv. 91/2, 237–246.

DEWEY, J. F. 1988: Extensional collapse of orogens. Tectonics 7/6, 1123–1139.

DUNNE, W. M. & HANCOCK, P. L. 1994: Paleo-stress analysis from small-scale brittle structures. In: HANCOCK, P. L. (Eds) Continental Deformation. Pergamon Press, Oxford, 101–120.

ESCHER, A. 1988: Structure de la nappe du Grand Saint-Bernard entre le val de Bagnes et les Mischabel. Service hydrol. et géol. national, 7, 26 p.

ESCHER, A., MASSON, H. & STECK, A. 1987: Coupes géologiques des Alpes occidentales suisses. Service Hydrol. Géol. National Suisse 2, 11 p.

ESCHER, A., HUNZIKER JOHANNES, C., MARTHALER, M., MASSON, H., SARTORI, M. & STECK, A. 1997: Geologic framework and structural evolution of the Western Swiss-Italian Alps. In: PFIFFNER, O. A., LEHNER, P., HEITZMAN, P., MUELLER, S. & STECK, A. (Eds.) Results of NRP 20; deep structure of the Swiss Alps. Birkhaeuser Verlag, Basel, 205–221.

GERLACH, H. 1883: Die penninischen Alpen. Beitr. Geol. Karte CH 27.

GRASEMANN, B. & MANCKTELOW, N. S. 1993: Two-dimensional thermal modelling of normal faulting; the Simplon fault zone, Central Alps, Switzerland. Tectonophysics 225/3, 155–165.

HANCOCK, P. L. 1985: Brittle micro-tectonics: Principles and practice. J. Struct. Geol. 7, 438–457.

HUBBARD, M. & MANCKTELOW, N. S. 1992: Lateral displacement during Neogene convergence in the Western and Central Alps. Geology 20/10, 943–946.

HUNZIKER, J. C., HURFOND, A. J. & CALMBACH, L. 1997: Alpine cooling and uplift. In: PFIFFNER, O. A., LEHNER, P., HEITZMAN, P., MUELLER, S. & STECK, A. (Eds.) Results of NRP 20; deep structure of the Swiss Alps. Birkhäuser Verlag, Basel, 260–263.

HURFOND, A. J. 1991: Uplift and cooling pathways derived from fission track analysis and mica dating: a review. Geol. Rdsch. 80, 349–368.

JEANBOURQUIN, P. & BURRI, M. 1989: La zone de Sion-Courmayeur dans la région du Simplon. Serv. Hydrol. Géol. National, Geol. Ber. 11, 35 p.

KASTRUP, U. 2002: Seismotectonics and stress field variations in Switzerland. PhD thesis, ETH-Zürich, 153 p.

KELLER, L. M. & SCHMID, S. M. 2001: On the kinematics of shearing near the top of the Monte Rosa nappe and the nature of the Furgg zone in Val Loranco (Antrona valley, N.Italy): tectonometamorphic and paleogeographical consequences. Schweiz. Mineral. Petrogr. Mitt. 81/3, 347–367.

LAUBSCHER, H. P. 1972: Some overall aspects of Jura dynamics. Amer. J. Sci. 272, 293–304.

– 1982: A northern hinge zone of the arc of the Western Alps. Eclogae Geol. Helv. 75/2, 233–246.

– 1988: Material balance in alpine orogeny. Geol. Soc. Amer., Bull. 100/9, 1313–1328.

– 1992: The Alps; a transpressive pile of peels. In: McClay, K. R. (Eds.) Thrust tectonics. Chapman & Hall, London, 277–285.

LUGEON, M. 1903: Les grandes dislocations et la naissance des Alpes suisses. Eclogae Geol. Helv. 7, 335–346.

MANCKTELOW, N. S. 1985: The Simplon Line: a major displacement zone in the western Lepontine Alps. Eclogae Geol. Helv. 78/1, 73–96.

– 1987: Quartz textures from the Simplon fault zone, Southwest Switzerland and North Italy. Tectonophysics 135/1–3, 133–153.

– 1990: The Simplon Fault Zone. Beitr. Geol. Karte CH 163 (n.F.), 74 p.

– 1992: Neogene lateral extension during convergence in the Central Alps; evidence from interrelated faulting and backfolding around the Simplon-pass; Switzerland. Tectonophysics 215/3–4, 295–317.

MANCKTELOW, N. S. & PAVLIS, T. L. 1994: Fold-fault relationships in low-angle detachment systems. Tectonics 13/3, 668–685.

MAURER, H. 1993: Seismotectonics and upper crustal structure in the Western Swiss Alps. PhD-thesis, ETH-Zürich, 159 p.

MAURER, H. R., BURKHARD, M., DEICHMANN, N. & GREEN, A. G. 1997: Active tectonism in the Central Alps; contrasting stress regimes north and south of the Rhone Valley. Terra Nova 9/2, 91–94.

MILNES, A. G. 1973: Structural Reinterpretation of the Classic Simplon Tunnel Section of the Central Alps. Geol. Soc. Amer., Bull. 84/1, 269–274.

– 1974: Post-nappe folding in the western Lepontine Alps. Eclogae Geol. Helv. 67, 333–348.

MOLNAR, P. & LYON-CAEN, H. 1988: Some simple physical aspects of the support, structure, and evolution of mountain belts. Spec. Paper Geol. Soc. Am. 218, 179–207.

NIEVERGELT, P., LINIGER, M., FROITZHEIM, N. & MAEHLMANN, R. F. 1996: Early to mid Tertiary crustal extension in the Central Alps; the Turba mylonite zone (eastern Switzerland). Tectonics 15/2, 329–340.

NIGGLI, E. 1975: Alpine Metamorphose und alpine Gebirgsbildung. In: ERNST (Ed.) Subduction zone metamorphism. Dowden, Hutchinson & Ross, Inc., Stroudsburg, Pa., U.S.A., 328–341.

PETIT, J. P. 1987: Criteria for the sense of movement on fault surfaces in brittle rocks. J. Struct. Geol. 9/5–6, 597–608.

PFIFFNER, O. A., LEHNER, P., HEITZMAN, P., MUELLER, S. & STECK, A. 1997: Results of NRP 20; Deep Structure of the Swiss Alps. Birkhäuser, Basel, 380 p.

PLATT, J. P., BEHRMANN, J. H., CUNNINGHAM, P. C., DEWEY, J. F., HELMAN, M., PARISCH, M., SHEPLEY, M. G., WALLIS, S. & WESTON, P. J. 1989: Kinematics of the Alpine arc and the motion history of Adria. Nature 337/6203, 158–161.

RAMSAY, J. G. & HUBER, I. M. 1987: The techniques of modern structural geology Vol. 2. Academic Press, London, 695 p.

RATSCHBACHER, L., FRISCH, W., NEUBAUER, F., SCHMID, S. M. & NEUGEBAUER, J. 1989: Extension in compressional orogenic belts: The eastern Alps. Geology 17, 404–40.

RATSCHBACHER, L., FRISCH, W., LINZER, H.-G. & MERLE, O. 1991: Lateral extrusion in the Eastern Alps; Part 2, Structural analysis. Tectonics 10/2, 257–271.

SCHMID, S., M., ZINGG, A. & HANDY, M. 1987: The kinematics of movements along the Insubric line and the emplacement of the Ivrea zone. Tectonophysics 135, 47–66.

SCHMIDT, C. 1907: Über die Geologie des Simplongebietes und die Tektonik der Schweizeralpen. Eclogae geol. Helv. 9, 484–584.

– 1908: Die Geologie des Simplongebirges und des Simplontunnels. Rectorats-Progr. Universität Basel. Friedrich Reinhard, Basel.

SCHMIDT, C. & PREISWERK, H. 1908: Geologische Karte der Simplongruppe, 1:50'000. Mit Verwertung der Aufnahmen von A. Stella. Mit Erläuterungen., Schweizerische Geologische Kommission, Geologische Spezialkarte 48.

SELVERSTONE, J. 1988: Evidence for east-west crustal extension in the Eastern Alps: implications for the unroofing history of the Tauern Window. Tectonics 7, 87–105.

SEWARD, D. & MANCKTELOW, N. S. 1994: Neogene kinematics of the central and western Alps: Evidence from fission-track dating. Geology 22/9, 803–806.

SOOM, M. A. 1990: Abkühlungs- und Hebungsgeschichte der Externmassive und der penninischen Decken beidseits der Simplon-Rhonelinie seit dem Oligozän: Spaltspurdatierungen an Apatit/Zirkon und K-Ar-Datierungen an Biotit/Muskowit. PhD thesis, Univ. Bern, 119 p.

STAMPFLI, G. M. & MARCHANT, R. H. 1997: Geodynamic evolution of the Tethyan margins of the Western Alps. In: PFIFFNER, O. A., LEHNER, P., HEITZMAN, P., MUELLER, S. & STECK, A. (Eds.) Results of NRP 20; deep structure of the Swiss Alps. Birkhäuser Verlag, Basel, 223–239.

STECK, A. 1984: Structures et déformations tertiaires dans les Alpes centrales. Eclogae Geol. Helv. 77/1, 55–100.

– 1987: Le massif du Simplon; reflexions sur la cinématique des nappes de gneiss. Schweiz. Mineral. Petrogr. Mitt. 67/1–2, 27–45.

STECK, A. & HUNZIKER, J. 1994: The Tertiary structural and thermal evolution of the Central Alps – compressional and extensional structures in an orogenic belt. Tectonophysics 238, 229–254.

STECK, A., EPARD, J. L., ESCHER, A., MARCHAND, R., MASSON, H. & SPRING, L. 1989: Coupe tectonique horizontale des Alpes centrales. Mém. Géol. Inst. Lausanne 5, 1–8.

STECK, A., EPARD JEAN, L., ESCHER, A., LEHNER, P., MARCHANT ROBIN, H. & MASSON, H. 1997: Geological interpretation of the seismic profiles through western Switzerland; Rawil (W1), Val d'Anniviers (W2), Mattertal (W3), Zmutt-Zermatt-Findelen (W4) and Val de Bagnes (W5). In: PFIFFNER, O. A., LEHNER, P., HEITZMAN, P., MUELLER, S. & STECK, A. (Eds.) Results of NRP 20; deep structure of the Swiss Alps. Birkhaeuser Verlag, Basel, 123–137.

STECK, A., BIGIOGGERO, B., DAL, P. G. V., ESCHER, A., MARTINOTTI, G. & MASSON, H. 1999: Carte tectonique des Alpes de Suisse occidentale et des régions avoisinantes 1:100'000, Landeshydrologie und -geologie, Carte Géol. Spéciale.

STECK, A., EPARD, J. L., ESCHER, A., GOUFFON, Y. & MASSON, H. 2001: Carte tectonique des Alpes de Suisse occidentale, Notice explicative. Landeshydrologie und -geologie, 73 p p.

SUE, C. & TRICART, P. 2002: Widespread post-nappe normal faulting in the internal Western Alps; a new constraint on arc dynamics. J. Geol. Soc. London 159/1, 61–70.

SUE, C., THOUVENOT, F., FRECHET, J. & TRICART, P. 1999: Widespread extension in the core of the western Alps revealed by earthquake analysis. J. Geophys. Res. B 104/11, 25611–25622.

TODD, C. S. & ENGI, M. 1997: Metamorphic field gradients in the central Alps. J. Met. Geol. 15, 513–530.

TRÜMPY, R. 1980: Geology of Switzerland – a guide-book. Part A: An outline of the geology of Switzerland. Part B: Geological excursions. Wepf, Basel, New York., 104 p.

VILLA, I. M. 1998: Isotopic closure. Terra Nova 10/1, 42–47.

VILLEMIN, T. & CHARLESWORTH, H. 1992: Stress, an interactive computer programm to determine paleostress axes using data from striated faults. Cordillera transect and cordilleran tectonic workshop,

WALLACE, R. E. 1951: Geometry of shearing stress and relation to faulting. J. Geol. 59/2, 118–130.

WAWRZYNIEC, T. F. & SELVERSTONE, J. 2001: Styles of footwall uplift along the Simplon and Brenner normal fault systems, central and Eastern Alps. Tectonics 20/5, 748–770.

WERNICKE, B. & BURCHFIEL, B. C. 1982: Modes of extensional tectonics. J. Struct. Geol. 4, 105–115.

Manuscript received March 10, 2003
Revision accepted March 29, 2004